Journal of the Taiwan Institute of Chemical Engineers 44 (2013) 758–761

Contents lists available at SciVerse ScienceDirect

Journal of the Taiwan Institute of Chemical Engineers

journal homepage: www.elsevier.com/locate/jtice

Highly textured ZnO:B films grown by low pressure chemical vapor deposition for efficiency enhancement of heterojunction silicon-based solar cells

Jui-Chung Hsiao [a,b], Chien-Hsun Chen [b,*], Hung-Jen Yang [c], Chien-Liang Wu [b], Chia-Ming Fan [b], Chien-Fu Huang [b], Chao-Cheng Lin [b], Peichen Yu [a], Jenn-Chang Hwang [c]

[a] Department of Photonics and Institute of Electro-Optical Engineering, National Chiao Tung University, HsinChu 30010, Taiwan
[b] Green Energy and Environment Research Laboratories, Industrial Technology Research Institute, HsinChu 30010, Taiwan
[c] Department of Materials Science and Engineering, National Tsing Hua University, Hsin-Chu City 30013, Taiwan

ARTICLE INFO

Article history:
Received 5 October 2012
Received in revised form 23 January 2013
Accepted 27 January 2013
Available online 30 March 2013

Keywords:
ZnO:B
Heterojunction solar cell
Low-pressure chemical-vapor-deposition

ABSTRACT

This paper demonstrates the growth of highly-textured boron-doped ZnO (ZnO:B) film by using low-pressure chemical-vapor-deposition (LPCVD) for efficient light harvesting and carrier collection in heterojunction silicon-based (HJS) solar cells. The optical and electrical characteristics have been optimized versus the substrate temperature and B_2H_6 flow rate for tradeoffs among the sheet resistance, free-carrier absorption, and optical transmission of blue/green wavelengths. A HJS solar cell with a 1.6-μm-thick ZnO:B film achieves a high power conversion efficiency of 16.30% and fill factor of 78.05%, compared to 15.64% and 72.17%, respectively, from a counterpart with a conventional 80-nm-thick indium tin oxide layer.

It is very important to have both a high energy conversion efficiency and a low production processing cost for commercialized solar cells. It is no doubt that the heterojunction silicon-based (HJS) solar cell is one of the most attractive solar cells among them for the following reasons [1–3]. First, the whole structure of a HJS solar cell is very simple. The emitter layer and the back-surface-filed (BSF) layer are deposited on a crystalline silicon (c-Si) substrate by a plasma enhanced chemical vapor deposition (PECVD) system. No sophisticated step, such as photolithography or ion-implantation, nor any complicated structure such as a metal wrap through or an inter-digital back contact is involved [4–6]. Second, the processing temperature of a HJS solar cell is very low. All of the required processes to a HJS solar cell can be accomplished below 250 °C using a PECVD system, which is especially suitable for thinner silicon wafers [7]. The reduction of the thermal budget, compared to the traditional crystalline silicon solar cell, is benefit to the mass production. Third, there is a very high energy conversion efficiency due to a high open voltage for a HJS solar cell [8]. An intrinsic hydrogenated amorphous silicon (a-Si:H) layer can be inserted between an emitter layer and a c-Si substrate or a BSF layer and a c-Si substrate, which can provide an excellent surface passivation to a c-Si substrate [9–11]. It is therefore attracted many people devoted on this topic.

Most of the research about HJS solar cells are focused on the intrinsic a-Si:H layer [9,12,10]. Only few papers discuss the transparent conductive oxide (TCO) layer on the HJS solar cells [13–16]. An Indium Tin Oxide (ITO) layer is a typical TCO material for the HJS solar cells. However, the shortage of the indium and free carrier adsorption at the long wave length region are two serious problems to an ITO material [17]. A ZnO-based TCO could be an alternative for its low cost and non-toxicity, attracting much attention for its widely applications to light-emitter diode, transparent high power electronics transducers, gas-sensing and solar cell [18,19]. It is an appropriate TCO layer for a HJS solar cell because it has the properties of a high transmittance (>80%) and a low sheet resistance (~10 Ω/□).

In this work, a ZnO:B layers were deposited by the low pressure chemical-vapor-deposition (LPCVD) system. The electrical and optical properties of ZnO films, which were controlled by the flow rate of the B_2H_6 and the substrate temperature, were optimized first. Second, the PV characteristics of HJS solar cells varying with the thickness of the optimized ZnO:B film from 0.35 μm to 1.6 μm were examined. Finally, the performance of HJS solar cells with the ZnO:B film and the ITO film, respectively, are discussed.

1. Experimental

The HJS solar cells were fabricated on textured n-type c-Si substrates cutting into 2 cm × 2 cm. The resistivity and thickness of the n-type CZ c-Si (1 0 0) substrates were 1–5 ? cm and 180 μm,

* Corresponding author. Tel.: +886 3 591 5170.
E-mail address: Tantalus@itri.org.tw (C.-H. Chen).

1876-1070/$ – see front matter
http://dx.doi.org/10.1016/j.jtice.2013.01.027

Table 1
The deposition parameters for the ZnO:B films used in this work.

ZnO:B sample	B_2H_6 (sccm)	Temperature (°C)	Pressure (Torr)	Sheet resistance (Ω/□)
#1	0	160	0.6	227
#2	3	160	0.6	11.2
#3	5	160	0.6	7.8
#4	10	160	0.6	6.3
#5	10	130	0.6	38
#6	10	200	0.6	125
#7	10	250	0.6	390
#8	10	300	0.6	353

respectively. Samples were dipped in 5% HF solution to remove the native oxide layer and then were rinsed in the de-ionized water in 3 min. A p-type a-Si:H film using B_2H_6 gas as a precursor and an n-type a-Si:H film using PH_3 gas as a precursor were deposited on a textured c-Si substrate as an emitter layer and a BSF layer. All ZnO:B films were deposited by LPCVD. Diethylzinc (DEZ) and water (H_2O) vapors carried by argon gas were used as precursors, and their flows were set to 500 and 550 sccm, respectively. Diborane (B_2H_6), 1% diluted in hydrogen, was used as the doping gas with the flow rate of 8 sccm. All the deposition parameters for ZnO:B films are summarized in Table 1. A silver grid layer, defined by a shadow metal mask, was sputtered on the ZnO:B film with a thickness of 200 nm. The Ag/ITO layers were sputtered on the n-type a-Si:H film as a back contact.

The electrical and optical properties of a ZnO:B film were characterized by four points probes and UV–vis spectrometer (Perkin Elmer, Lambda 750s). Scanning electron microscope (JEOL, JSM 5400) was utilized to investigate the surface morphology and thickness of a ZnO:B film. The photovoltaic characteristics of the HJS solar cells were determined under standard illumination test condition (25 °C, 1000 W/m^2, AM 1.5 G).

2. Results and discussion

Fig. 1 shows the sheet resistance ($R_\square$) of the ZnO:B films as a function of the diborone (B_2H_6) dilution. There is a drastic decrease of the $R_\square$ from 227 Ω/□ to 11.2 Ω/□ with the increase of the B_2H_6 from 0 sccm to 3 sccm. The $R_\square$ can be further decreased to 7.8 Ω/□ at the B_2H_6 flow rate of 5 sccm and seems to be saturated to 6.3 Ω/□ at the B_2H_6 flow rate of 10 sccm. Both electrical and optical properties are important to the transparent conductive layer. The transmission of the ZnO:B films with different B_2H_6 flow rate are

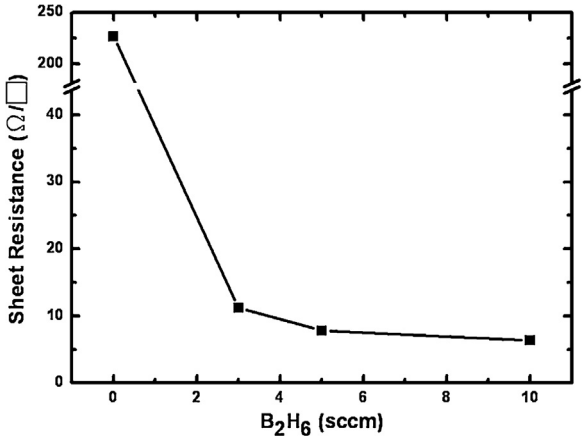

Fig. 1. The measured sheet resistance value of the ZnO:B films as a function of the diborone dilution.

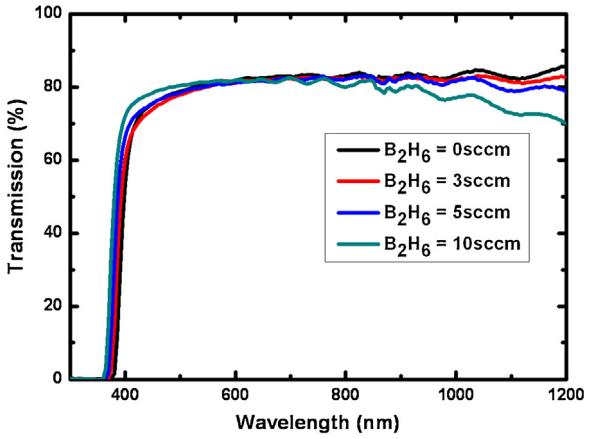

Fig. 2. The transmission of the ZnO films with different B_2H_6 dilution from the spectrometer.

measured from the wavelength of 300 nm to 1200 nm (Fig. 2). There is a blue-shift of a cut-off wavelength for the ZnO:B films in the ultra-violet region increasing with the B_2H_6 flow rate. This is mainly due to the Burstein Moss shift [20]. The transmissions are also increased with the B_2H_6 flow rate at these wavelength ranges. On the contrary, the transmissions of these ZnO:B films are decreased with the increase of the B_2H_6 flow rate in the IR region. This can be attributed to the free electrons adsorption at the long wavelength region [17]. Meanwhile, the transmissions are almost the same (~80%) at the wavelength of 550–850 nm for the all ZnO:B samples regardless of the B_2H_6 flow rate.

It is noted that the deposition rate and the orientation of the ZnO:B films, determined by the SEM and XRD, respectively, are not affected by the B_2H_6 flow rate from 0 sccm to 10 sccm. On the contrary, the increase of the substrate temperature has remarkable change in the surface morphology as shown in Fig. 3. The structures of the ZnO:B films change from granular-like structure at 130 °C to pyramid-like structure at 160 °C and further change to stripe-like structure at 300 °C deposited on the textured silicon substrate. More importantly, the lowest $R_\square$ can be obtained to be ~6.3 Ω/□ at 160 °C as shown in Table 1.

It is important to take the optical and electrical properties of the ZnO:B films as well as the deposition temperature into the consideration for the fabrication of the HJS solar cells. The B_2H_6 flow rate and the deposition temperature are chosen to be 10 sccm and 160 °C, respectively. Generally speaking, the optimized thickness of an ITO film for a HJS solar cell is 80 nm. It is noted that the resistivity of a ZnO:B film (~4×10^{-3} Ωcm) is higher than that of an ITO film (~3×10^{-4} Ωcm). The optimized thickness of a ZnO:B film for a HJS cell should be larger than 80 nm. The thickness of the ZnO:B films are varied from 0.35 μm to 1.6 μm to investigate how they affect the PV characteristics, including open circuit voltage (V_{oc}), short circuit current density (J_{sc}), fill factor (FF), and energy conversion efficiency (Eff.) of the HJS solar cells as shown in Fig. 4. The J_{sc} values of HJS solar cells with ZnO:B films are almost the same at the ZnO:B films thickness of 0.35 μm and 0.8 μm, but decrease rapidly to 35.2 mA/cm^2 as the thickness of the ZnO:B film rises to 1.6 μm. There is a relation between the incident light (I_0) and the transmission light (I):

$$I = I_0 e^{(-\alpha t)} \quad (1)$$

where α and t are the absorption coefficient and thickness of the film, respectively. The intensity of the transmission light is inversely exponential to the thickness of the film, suggesting that the J_{sc} decreases with the increase of the film thickness. The

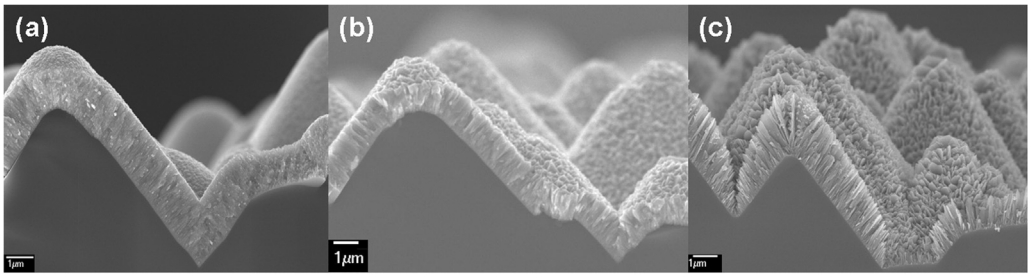

Fig. 3. The SEM cross sections of ZnO:B films deposited on c-Si in (a)130 °C, (b)160 °C and (c)300 °C.

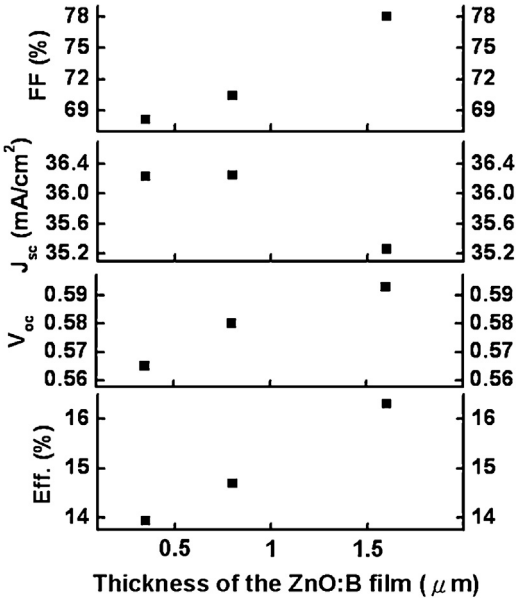

Fig. 4. Photovoltaic characteristics of (a) fill factor, FF (b) short circuit current density, J_{sc} (c) open circuit voltage, V_{oc} and (d) conversion efficiency, Eff. for HJS solar cells as a function of the thickness of the ZnO:B film and for a HJS solar cell with the ITO film (blue spot).

quantum efficiencies (QEs) of HJS solar cells with different thickness of the ZnO:B flms as shown in Fig. 5 can further explain this phenomenon. The major difference in QEs for these HJS cells is at the wavelength of 600–1200 nm, in which the QE of the HJS cell with the ZnO:B film of 1.6 μm thick is smaller than that with the ZnO:B film of 0.8 μm. The HJS cell has high energy conversion

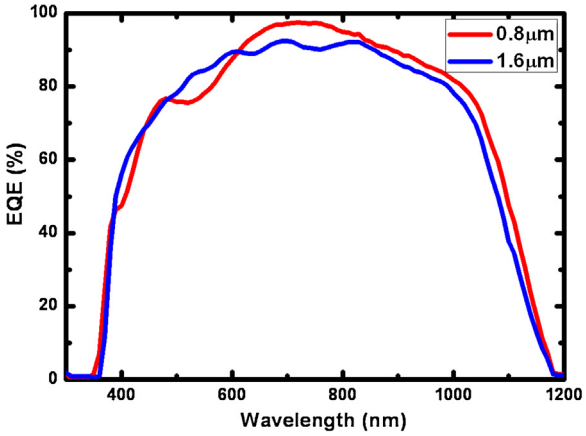

Fig. 5. The quantum efficiency of HJS solar cells for two ZnO:B films with thickness of 0.8 μm and 1.6 μm.

Table 2
Photovoltaic characteristics of open circuit voltage (V_{oc}), short circuit current density (J_{sc}), fill factor (FF), and conversion efficiency (Eff.) for HJS solar cells with the ITO film and the ZnO:B film.

Sample	V_{oc} (V)	J_{sc} (mA/cm^2)	FF (%)	Eff. (%)
HJS cell with the ITO film	0.593	36.51	72.17	15.64
HJS cell with the ZnO:B film	0.593	35.26	78.05	16.3

efficiency at the long wavelength region because the bandgap of the silicon is 1.1 eV. As a consequence, the thicker the ZnO:B film, the lower the J_{sc}.

The FFs values of HJS solar cells with ZnO:B layers increases by a factor of 1.14 with the increase of the thickness of the BZO film from 0.35 μm to 1.6 μm. It can be originated from the film thickness effect because the $R_{\square}$ is inversely proportional to the film thickness, which results in the larger FF. Furthermore, a smaller $R_{\square}$ can result in a lower series resistance, leading to a higher V_{oc} value. This explains the FF and V_{oc} increasing with the thickness of the ZnO:B film.

The efficiency results combine with total factors including the FF, V_{oc}, and J_{sc}. The tendency of efficiency of HJS solar cells is the same as the FF results. The optimized efficiency of 16.2% can be obtained at the ZnO:B layer thickness of 1.6 μm.

In most HJS solar cell research, an ITO film is chosen as a transparent conductive oxide layer because of its excellent optical and electrical properties. It is of interest to compare the PV characteristics between HJS solar cells with an ITO film of 80 nm thick and a ZnO:B film of 1.6 μm thick, respectively, as shown in Table 2. The FF of the HJS solar cell with a ZnO:B film is higher than that with an ITO film, because the $R_{\square}$ of 6.3 Ω/□ for a ZnO:B film is lower than the $R_{\square}$ of 50 Ω/□ for an ITO film. Meanwhile, the thicker film results in a lower J_{sc} as mentioned earlier. It is worth noting that the most significant feature of the low pressure chemical vapor deposited ZnO:B film is the textured structure (Fig. 3), which is benefit to the light absorption and contributes to the J_{sc} of the solar cell. Otherwise, the J_{sc} would be lower than we measured. There are two main disadvantages for an ITO film thicker than 80 nm. One is that the J_{sc} will decrease due to the absorption of the thicker film. The other is that the absorption at the long wavelength region increases rapidly because of the free carrier absorption [17,21].

3. Conclusions

We have fabricated the HJS solar cells using ZnO:B films as the TCO material deposited by an LPCVD system. Due to its high transmittance, low sheet resistance as well as the textured structure, the higher energy conversion efficiency of the HJS solar cell was obtained than that with an ITO film as the TCO layer. Other works such as the improvements of the optical and electrical properties of the ZnO:B films on the HJS solar cells are in process.

Acknowledgements

This work was supported by Bureau of Energy under the contract No. B455DR1120.

References

[1] Qi W, Page MR, Iwaniczko E, Yueqin X, Roybal L, Bauer R, et al. Efficient heterojunction solar cells on p-type crystal silicon wafers. Appl Phys Lett 2010;96:013507.
[2] Takahiro M, Mikio T, Hitoshi S, Eiji M. Development status of high-efficiency HIT solar cells. Sol Energy Mater Sol Cells 2011;95:18–21.
[3] Hiroyuki F, Tetsuya K, Michio K. Optimization of interface structures in crystalline silicon heterojunction solar cells. Sol Energy Mater Sol Cells 2009;93:725–8.
[4] Clement F, Menkoe M, Erath D, Kubera T, Hoenig R, Kwapil W. *et al.* High throughput via-metallization technique for multi-crystalline metal wrap through (MWT) silicon solar cells exceeding 16% efficiency. Sol Energy Mater Sol Cells 2010;94:51–6.
[5] Guillevin N, Geerligs LJ, Naber RCG, Eerenstein W, Weeber AW. High efficiency n-type metal wrap through Si solar cells for low-cost industrial production. In: 25th EU-PVSEC 2010; 2DO.1.4; 2010.
[6] Woehl R, Krause J, Granek F, Biro D. 19.7% efficient all-screen-printed back-contact back-junction silicon solar cell with aluminum-alloyed emitter. IEEE Electron Device Lett 2011;32:3.
[7] Yasufumi T, Yukihiro Y, Mikio T, Toshiaki B, Toshihiro K, Hiroshi K. *et al.* Twenty-two percent efficiency HIT solar cell. Sol Energy Mater Sol Cells 2009;93:670–3.
[8] Mikio T, Akira T, Eiji M, Makoto T. Obtaining a higher V_{oc} in HIT cells. Prog Photovolt Res Appl 2005;13:481.
[9] Wang TH, Iwaniczko E, Page MR, Levi DH, Yan Y, Branz HM, et al. Effect of emitter deposition temperature on surface passivation in hot-wire chemical vapor deposited silicon heterojunction solar cells. Thin Solid Films 2006;501:284.
[10] Das UK, Burrows MZ, Lu M, Bowden S, Birkmire RW. Surface passivation and heterojunction cells on Si (1 0 0) and (1 1 1) wafers using dc and rf plasma deposited Si:H thin films. Appl Phys Lett 2008;92:063504.
[11] Mikio T, Kunihiro K, Sadaji T, Toshiaki B, Hitoshi S, Masashi M, et al. HIT™ cells-high-efficiency crystalline Si cells with novel structure. Prog Photovolt Res Appl 2000;8:503.
[12] Hiroyuki F, Michio K. Impact of epitaxial growth at the heterointerface of a-Si:H/c-Si solar cells. Appl Phys Lett 2007;90:013503.
[13] Favier A, Munoz D, Martin de Nicolas S, Ribeyron P-J. Boron-doped zinc oxide layers grown by metal-organic CVD for silicon heterojunction solar cells applications. Sol Energy Mater Sol Cells 2011;95:1057.
[14] Koida T, Fujiwara H, Kondo M. High-mobility hydrogen-doped In2O3 transparent conductive oxide for a-Si:H/c-Si heterojunction solar cells. Sol Energy Mater Sol Cells 2009;93:851.
[15] Choong G, Bole P, Barraud L, Zicarelli F, Descoeudres A, de Wolf S, et al. Transparent conductive oxides for silicon heterojunction solar cells. In: Proc. 25th Europ. Photovoltaic Solar Energy Conf. 2010; 2DV.1.25; 2010.
[16] Zhao L, Zhou CL, Li HL, Diao HW, Wang WJ. Role of the work function of transparent conductive oxide on the performance of amorphous/crystalline silicon heterojunction solar cells studied by computer simulation. Phys Stat Sol (a) 2008;205:1215–21.
[17] Faÿ S, Steinhauser J, Nicolay S, Ballif C. Polycrystalline ZnO:B grown by LPCVD as TCO for thin film silicon solar cells. Thin Solid Films 2010;518:2961.
[18] Huang J-B, Nam Giang N, Chou C-H, Wei S-S, Hong L-S. Nitride-based LEDs fabricated on ZnO-buffered sapphire substrates. J Taiwan Inst Chem Eng 2012;43:638–43.
[19] Pearton SJ, Norton DP, Ip K, Heo YW, Steiner T. Recent progress in processing and properties of ZnO. Prog Mater Sci 2005;50:293–340.
[20] Lee GH, Yamamoto Y, Kourogi M, Ohtsu M. Blue shift in room temperature photoluminescence from photo-chemical vapor deposited ZnO films. Thin Solid Films 2001;386:117.
[21] Kang D-W, Kuk S-H, Ji K-S, Lee H-M, Han M-K. Effects of ITO precursor thickness on transparent conductive Al doped ZnO film for solar cell applications. Sol Energy Mater Sol Cells 2011;95:138.